



Original Article

Efficient methylene blue dye removal using hybrid ZnO/Co/Cs photocatalyst beads



Kwang Zhean Ong¹, Mohd Fadhil Majnis^{2,*} , Mohd Azam Mohd Adnan³ , Suhanna Natalya Mohd Suhaimy¹ 

¹ Department of Chemical and Petroleum Engineering, Faculty of Engineering, UCSI University, 56000, Kuala Lumpur, Malaysia

² School of Chemical Engineering, College of Engineering, Universiti Teknologi MARA, 40450, Shah Alam, Selangor, Malaysia

³ Advanced Materials & Manufacturing Research Group (AMMRG), Faculty of Engineering and Life Sciences, University of Selangor, 45600, Bestari Jaya, Selangor, Malaysia

* Correspondence email: fadhilmajnis@uitm.edu.my

Abstract

This study highlighted the developments of the hybrid photocatalytic system for wastewater treatment in the textile industry. Chitosan (Cs) and cobalt (Co) were introduced into the conventional catalyst zinc oxide (ZnO) to form the hybrid photocatalyst beads. Four different weight ratios of ZnO/Cs (1:1) and ZnO/Co/Cs (1:1:1, 1:2:1 and 2:1:1) beads were synthesized by the sol-gel method. The photocatalytic degradation properties of the hybrid ZnO/Co/Cs were investigated under visible light irradiation for methylene blue (MB) photodegradation. The study focused on the effect of ZnO/Co/Cs composition ratio, irradiation time and the amount of catalyst loading in the photoreactor for five hours of exposure time. The result was that the 1:1:1 ZnO/Co/Cs photocatalyst beads had the highest degradation rate compared to the other systems. Adding Co to the ZnO/Cs photocatalyst improved the photocatalytic activity by increasing the decolourization percentage of methylene blue.

Copyright © 2024 PENERBIT AKADEMIA BARU - All rights reserved

Article Info

Received 13 July 2023

Received in revised form 27 November 2023

Accepted 10 January 2024

Available online 15 January 2024

Keywords

Azo dye
Photocatalytic
Zinc oxide
Cobalt
Chitosan

1 Introduction

Methylene blue (MB) is a cationic thiazine dye characterized by a thiazine ring in its molecular structure. The dye molecule typically derives the positive charge from amino or quaternary ammonium groups [1,2]. It is widely used in various industries as a biological stain and chemical indicator [3] and as dyes in cotton, leather, paper, textile, mordant, and plastic industries [4]. Under certain circumstances, it can be hazardous, carcinogenic, mutagenic, and ecologically persistent [5]. Therefore, thiazine dyes need to be removed during wastewater treatment. There are some efficient methods to remove thiazine dyes, such as physical adsorption [4,6], oxidation [7,8], electrochemical degradation [9,10] and photocatalytic degradation [11,12]. However, some methods are unstable, harmful, can cause corrosion reactions, and are expensive. Among these methods, photocatalytic degradation seems to be the most useful because it uses a non-toxic, stable compound with high efficiency in removing pollutants [13]. It is inexpensive due to the chemical compound and maintenance. In the current research on photocatalytic degradation, semiconductor photocatalysts are used under light irradiation to destroy dye compounds.

Zinc oxide (ZnO) is recognized as a promising photocatalyst due to its unique advantages, high catalytic activity, low cost, and high stability. This compound is an excellent catalyst for the photooxidation of organic pollutants, in which it absorbs UV light via electronic excitation between the valence and conduction bands [14]. Zinc oxide absorbs light energy, and the amount of energy absorbed is greater than or equal to the band gap of the photocatalyst. The band gap of ZnO is approximately 3.34 eV. However, the high recombination of the photons produced results in a large band gap, which limits or hinders practical applications to some extent. In addition, there is a photoexcited step to the conduction band on an empty state for each electron, creating an overlapping oxygen 2p orbital that forms a valence band. The higher the band gap, the more empty states are created in the orbital, and more energy is consumed. This condition later affects the adsorption rate of the photocatalyst to the pollutant. Accordingly, several methods are being investigated to reduce the band gap. One of these methods is doping the photocatalyst with a transition metal. Doping with transition metal promotes photoreaction by changing the original photocatalyst's physical properties and reducing the band gap. The metal sites act as trapping sites by accepting the photogenerated electrons or holes from the photocatalyst. This situation limits the recombination of the charge carriers and improves the photocatalytic activity [15,16]. Among the transition metals, cobalt (Co) was chosen as the transition element for doping ZnO because it is one of the most effective species for tuning electronic and optical properties. In addition, Co has a minimal effect on the ZnO lattice structure, so the physical properties of ZnO are not affected. When ZnO is doped with Co, there is a sudden change in the band gap of ZnO. A negative and positive correction of the conduction band and the valence band edge leads to a narrowing of the band gap. Thus, the photogenerated electron of ZnO/Co can be easily transferred from the valence band of ZnO to the energy level of the localized dopant. A band will exist between ZnO and Co, which will eventually support the doping of Co into ZnO, benefiting the effectiveness of separation and transport of photogenerated electrons in the catalyst [15, 17].

In addition, it has been reported that incorporating chitosan (Cs) into semiconductor photocatalysts can adsorb heavy metals, organic and inorganic pollutants. These properties are mainly due to the high amino (-NH₂) and hydroxyl groups (-OH) content in the polymer matrix, which can serve as coordination and reaction sites for adsorption. Chitosan is a deacetylated derivative of chitin obtained from the exoskeleton of shellfish such as shrimps, crabs and prawns. Chitosan is a semi-crystalline polymer that contains inter- and intramolecular hydrogen bonds that reduce its solubility properties in organic solvents and dilute acids [18], [19–22]. Chitosan has versatile physical and chemical properties and is well tolerated due to its cationic nature, compatibility, and non-toxicity.

Consequently, in the present study, the ZnO was combined with Cs and Co to synthesize ZnO/Co/Cs beads using the sol-gel method, to fulfil its dual role as an excellent absorbent and photocatalyst. The sol-gel technique is a chemical procedure widely adapted for creating different nanostructures. In this technique, the molecular precursor is dissolved in water or alcohol, followed by heating and stirring to form a gel, a process known as hydrolysis or alcoholysis. The other key advantages of adopting the sol-gel technique are high purity, narrow particle size dispersion, and the ability to generate homogeneous nanostructures at low temperatures [23]. These hybrid ZnO/Co/Cs beads are hoped to be a valuable photocatalyst that can be used in water treatment, especially in removing dyes. The article deals with the synthesis of hybrid ZnO/Co/Cs beads and their photocatalytic activity against the MB dye under visible light at different conditions, such as different compositions of ZnO/Co/Cs, ZnO/Co/Cs dosage and irradiation time.

2 Experiments

2.1 Materials

The zinc acetate dihydrate with an empirical formula of Zn(CH₃COO)₂·2H₂O with a purity of more than 95% was used to synthesize zinc oxide powder. Meanwhile, the reagent grade of cobalt (II) acetate tetrahydrate with an empirical formula of (CH₃COO)₂Co·4H₂O was used as a co-catalyst with zinc oxide. Methylene blue with an empirical formula of C₁₆H₁₈ClN₃S was used as the model dye. It is a well-known and easily measurable dye, allowing for accurate monitoring of its degradation and oxidation processes [24,25]. The moderate molecular weight chitosan (C₁₂H₂₄N₂O₉) flakes were utilized

as catalyst support for both photocatalysts. All chemicals, including acetic acid, ethanol, and sodium hydroxide, were bought from Sigma-Aldrich and used without further purification. All standard solutions are washed, cleaned, and prepared using deionized (DI) water. A synthetic dye solution of MB with a concentration of 1000 mg/L was prepared as a stock solution for subsequent dilution.

2.2 Formation of hybrid photocatalyst using Sol-Gel method

2.2.1 Synthesis of ZnO powder

Zinc acetate dihydrate was weighed 4.38 g before being dissolved in 100 ml of ethanol. The mixture was then stirred for about 2 hours. Later, 15 ml of 0.5 M sodium hydroxide (NaOH) was titrated into the solution after stirring for 2 hours. After titrating sodium hydroxide into the mixture, the mixture was stirred further for about one hour until the mixture turned a completely chalky white colour. The mixture was then filtered with filter paper. The filtered substances were then dried in an oven for 2 hours at 120 °C. After the drying process, the sample was ground into powder form. The powdered zinc oxide (ZnO) was calcined in an oven for 3 hours at 600 °C. Calcining helps to remove impurities and moisture from the ZnO powder, resulting in a pure and more stable product [26,27].

2.2.2 Synthesis of ZnO/Co powder

One gram of zinc oxide powder and 1 g of cobalt (II) acetate tetrahydrate were mixed with 80 mL of ethanol to give a 1:1 weight ratio of ZnO to Co. The mixture was then stirred for about 48 hours. The mixture was then oven-dried at 100 °C for about 12 hours. After drying, the remaining residue was zinc oxide and cobalt in crystal form. The dried 1:1 mixture of zinc oxide and cobalt (II) acetate tetrahydrate was ground to obtain ZnO/Co hybrid catalyst powder. The processes were repeated for 1:2 and 2:1 ZnO/Co hybrid catalyst mixing ratios.

2.2.3 Preparation of chitosan solution

One gram of chitosan powder was dissolved in 30 ml of 2% acetic acid. The solution was stirred at 250 rpm for 4 hours. Then, another 20 ml of acetic acid was added to the solution to dissolve the chitosan completely. Acetic acid as a solvent for chitosan facilitates the composite creation of chitosan with other matrices, such as metal oxide, causing notable alterations in the chitosan polymeric chemistry [28].

2.2.4 Formation of ZnO/Co/Cs photocatalyst beads

The synthesized 1:1 ZnO/Co (1 g ZnO and 1 g Co) was mixed with 1 gram of prepared chitosan solution. Both mixtures were stirred for about 3 hours at a temperature of 25 °C to ensure that the solution was homogeneously mixed. Then, the solution was extracted and slowly dropped into the 0.5M sodium hydroxide (NaOH) solution using a syringe pump to form ZnO/Co/Cs beads. NaOH neutralizes the photocatalyst beads made of chitosan powder dissolved in acetic acid [29]. The NaOH neutralization process ensures that the photocatalyst beads are stable and usable as photocatalysts for dye degradation. The beads formed in the NaOH solution were then transferred to fresh NaOH and allowed to stand for 24 hours to ensure that the beads were stable and did not break during photocatalytic activity. Later, the beads were filtered and washed several times until pH7 was reached to remove excess NaOH. After washing the beads, the sample was kept in a container filled with DI water. The processes were repeated for 1:2 and 2:1 ZnO/Co to produce 1:2:1 (1 g ZnO: 2 g Co: 1 g chitosan solution) and 2:1:1 (2 g ZnO: 1 g Co: 1 g chitosan solution) ZnO/Co/Cs photocatalyst beads.

2.3 Photocatalytic activity

The photocatalytic activity was carried out using a photoreactor, as shown in Fig. 1, where 80 ml of 10 ppm methylene blue was added to a beaker and placed in the photoreactor. The bubble was introduced into the beaker through the tubing connected to a pump. The kinetics for removing the dye from the aqueous solution were carried out at different time intervals, namely 0, 1, 2, 3, 4 and 5 hours. In the experiments on photodegradation, the extent of decolourization of the dye in per cent was calculated using the following equation:

$$\text{Decolourization (\%)} = \frac{C_0 - C_t}{C_0} \times 100 \quad (1)$$

where C_o is the initial concentration of dye (mg/L), and C_t is the concentration of dye (mg/L) at an interval time.

2.4 Scanning electron microscopy analysis

Scanning electron microscopy, model FEI Quanta 200 FESEM was used to analyze the morphological structure of the ZnO/Co/Cs photocatalysts. The ZnO/Co/Cs were dried before being viewed at SEM at various magnifications.

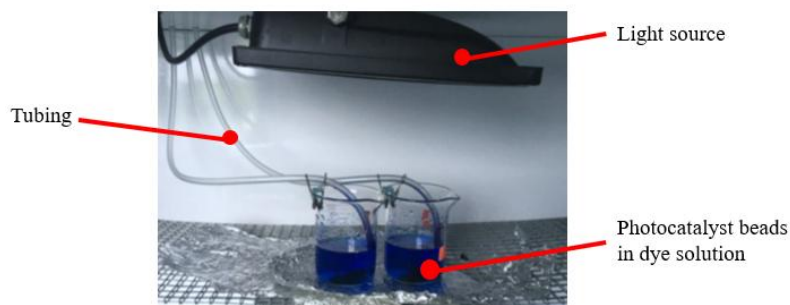


Fig. 1 Arrangement in photoreactor for degradation of methylene blue using ZnO/Cs and ZnO/Co/Cs photocatalyst beads.

3 Results and Discussion

3.1 Formation of ZnO/Co/Cs beads

Fig. 2 shows the synthesized ZnO/Co/Cs photocatalyst beads. The ZnO/Co/Cs beads were formed using a dropwise method into NaOH solution as a solidification solution, as shown in Fig. 2(a). In the initial phase, the colourless beads precipitate and turn pink after a few minutes, as shown in Fig. 2(b). The formed beads progress and slowly turn blackish brown after 24 hours. A similar development was also reported by Gueli et al. [30]. The beads were soaked in sodium hydroxide for several hours and stored to stabilize their structure, as they are very fragile and can easily break during photocatalytic activity in the photoreactor. Notably, all the different ratios of the ZnO/Co/Cs catalyst (1:1:1, 1:2:1 and 2:1:1) resulted in a similar formation. It should be noted that using chitosan improved the adsorption properties and increased the degradation efficiency. Since chitosan has excellent properties concerning the individual components, it has a remarkable synergistic effect. It can form a metal compound with zinc oxide due to the NH_2 group and the OH groups [31].

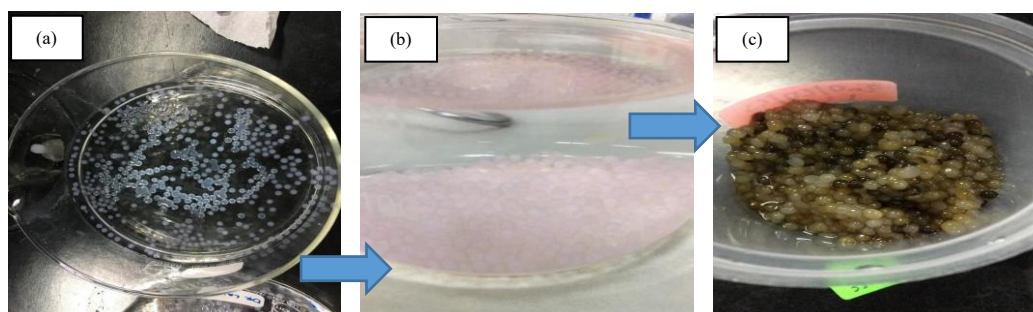


Fig. 2 Formed ZnO/Co/Cs photocatalyst beads.

3.2 Surface morphology of ZnO/Co/Cs

Fig. 3 shows the SEM images of the ZnO/Co/Cs in powder form with different magnifications. The flower-like structure and other aggregated structures visible in Fig. 3(c) confirm the presence of ZnO and Co. ZnO and Co are probably combined within the Cs in the ternary system of the composite [32].

Certain materials have an inherent propensity to self-organize into specific formations due to their surface energy and intermolecular forces [33]. During the mixing procedure, these materials can arrange themselves into complex configurations such as flower-like structures. The SEM images also show the inhomogeneous agglomerated surface and the gaps in the surface morphology of ZnO/Co/Cs. The higher magnification in Fig. 3(d) shows the porous structure. The presence of Cs is thought to play a crucial role in forming and controlling ZnO and Co nanoparticles. These nanoparticles can attach to CS molecules during synthesis, leading to pore formation. Moreover, CS has a porous structure that contributes to this phenomenon [33]. Interactions between different ZnO and Co molecules on the nanoscale also contribute to the formation of pores. The process of Ostwald ripening could be another explanation for this phenomenon. In this process, smaller particles dissolve and redeposit on larger particles, creating voids and pores in the overall structure [34].

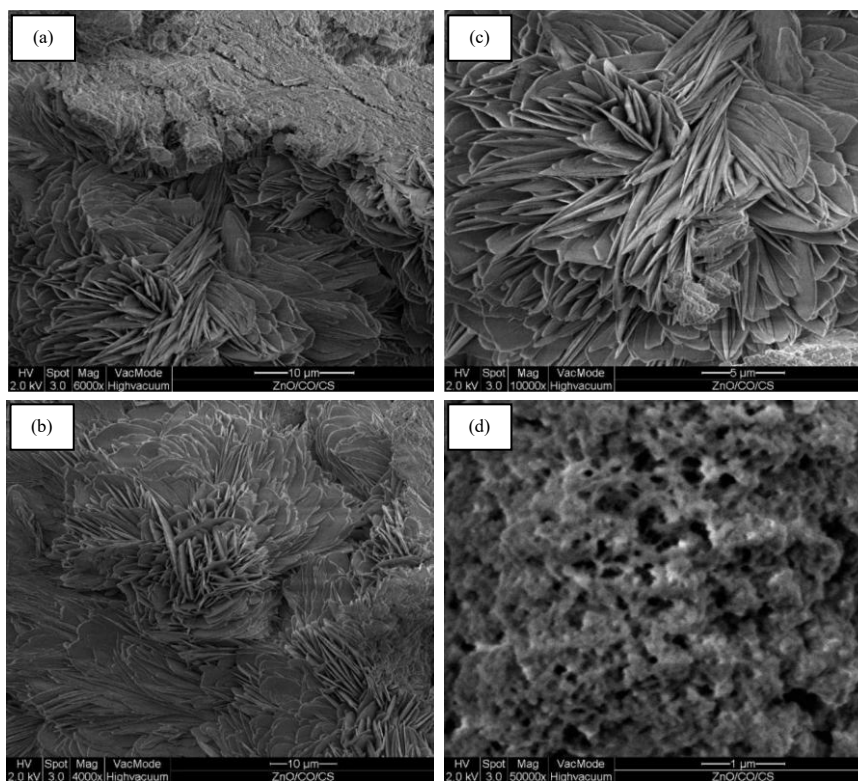


Fig. 3 SEM images of ZnO/Co/Cs (1:1:1) at various magnifications.

3.3 Evaluation of photocatalytic properties

3.3.1 Effect of the composition ratio of ZnO/Co/Cs

The composition ratio of ZnO/Co/Cs has been divided into four different compositions. These are 1:0:1, 1:1:1, 1:2:1 and 2:1:1. Table 1 shows the decolourization percentage of methylene blue at various compositions of ZnO/Co/Cs photocatalyst beads. Observation after 5 hours at an interval of 1 hour each showed that the photocatalytic activity of 1:1 ZnO/Cs beads did not decrease much, especially with a small amount of ZnO/Cs beads. The results showed 38.3% and 36.98% percentage decolourization for 1 g and 2 g of 1:1 ZnO/Cs beads, respectively, indicating little change in the presence of photon energy. However, significant photocatalytic activity was observed when the amount of 1:1 ZnO/Cs beads was increased to 3 g, corresponding to about 55.15 % of decolourization. Adding Co to the ZnO/Cs catalyst (1:1:1 and 1:2:1 of ZnO/Co/Cs) improved the decolourization of methylene blue compared to a catalyst without Co (1:1 of Zn/Cs). With increasing Co ratio, 1:1:1 and 1:2:1 of ZnO/Co/Cs beads, methylene blue's photocatalytic degradation was varied by adding 1 g and 2 g of ZnO/Co/Cs beads. However, 3 g of ZnO/Co/Cs beads was sufficient to increase the decolourization percentage of methylene blue. After 5 hours of light exposure, the results showed 55.15%, 79.29% and 83.59% decolourization for 1:1 of

ZnO/Cs bead, 1:1:1 and 1:2:1 of ZnO/Co/Cs beads, respectively. It is believed that adding Co alters the band gap of the ZnO/Co/Cs beads and thus improves the photocatalytic properties. Y. Lu et al. [15] also reported a similar finding. Moreover, the decolourization percentage was decreased with an increasing ratio of ZnO, i.e. 1:1:1 and 2:1:1 ZnO/Co/Cs beads.

Table 1 Photocatalytic degradation of Methylene Blue using (a) 1:1 of ZnO/Cs, (b) 1:1:1 ZnO/Co/Cs, (c) 1:2:1 ZnO/Co/Cs and (d) 2:1:1 ZnO/Co/Cs

Exposure Time (hours)	1:1 of ZnO/Cs		
	Decolourization (%)		
	1g	2g	3g
0h	11.30	13.69	14.96
1hr	28.18	27.54	46.29
2hr	30.56	32.04	49.95
3hr	37.69	34.09	52.32
4hr	37.88	34.67	52.58
5hr	38.26	36.98	55.15

(a)

Exposure Time (hours)	1:2:1 ZnO/Co/Cs		
	Decolourization (%)		
	1g	2g	3g
0h	16.69	19.24	41.65
1hr	44.36	44.68	78.97
2hr	45.07	45.45	79.67
3hr	47.64	45.65	80.89
4hr	48.66	48.28	80.96
5hr	52.52	52.39	83.59

(b)

Exposure Time (hours)	1:1:1 of ZnO/Co/Cs		
	Decolourization (%)		
	1g	2g	3g
0h	12.33	14.32	16.69
1hr	22.08	59.90	68.24
2hr	24.27	62.66	69.59
3hr	26.13	63.24	73.89
4hr	26.13	63.56	78.26
5hr	27.09	66.19	79.29

(c)

Exposure Time (hours)	2:1:1 of ZnO/Co/Cs		
	Decolourization (%)		
	1g	2g	3g
0h	10.91	12.71	13.72
1hr	23.05	39.23	51.94
2hr	30.05	41.34	54.95
3hr	30.05	42.05	61.95
4hr	32.74	42.18	66.64
5hr	40.51	42.76	68.89

(d)

3.3.2 Effect of catalyst loading

Catalyst loading could affect degradation activity. In this study, the photocatalytic activity was carried out with three different loadings, namely 1 g/L, 2 g/L and 3 g/L ZnO/Co/Cs photocatalyst beads. Table 1 shows that methylene blue degradation increased significantly with the higher loading of the ZnO/Co/Cs photocatalyst. At 1:1 Zn/Cs, 1:1:1, 1:2:1 and 2:1:1 Zn/Co/Cs mixing ratios of the ZnO/Co/Cs photocatalyst, the percentage of methylene blue decolourization increased with increasing catalyst loading. However, for 1:1 ZnO/Cs, the decolourization percentage decreased when the catalyst loading was increased up to 2 g and increased when the loading was up to 3 g. It can be concluded that the 3 g ZnO/Co/Cs photocatalyst showed a remarkable result in all different ratios. As compared to the work by Farzana and Meenakshi [18, 22], they used a varied zinc oxide-impregnated chitosan beads catalyst dose of 1g/L, 1.5 g/L, 2 g/L, 2.5 g/L and 3 g/L for methylene blue and rhodamine B removal. Similar to current work, results show that the photocatalyst loading increases and the reaction occurs faster due to many active sites on the photocatalyst. On the other hand, the percentage of decolourization decreases beyond the limit of 2 g/L in their work. It is due to the increasing turbidity of the suspension, which obstructs the path of light to the dye molecules.

3.3.3 Effect of irradiation time

In this study, the effect of irradiation time on the decolourization of methylene blue was investigated at different time intervals from 0 to 5 hours. The normalized temporal concentration changes (C/C_0) of methylene blue during photodegradation were derived from the absorbance (A/A_0). Table 1 shows that the percentage decolourization with 1:2:1 ZnO/Co/Cs had significantly higher photocatalytic activity when 3 g of catalyst was used. It was found that the percentage of decolourization in all composition

ratios of ZnO/Co/Cs increased with increasing time. With increasing time, more light energy falls on the catalyst's surface. This situation leads to increased formation of light-released species and increases the photocatalytic activity. The apparent reaction constant of photocatalytic decolourization was calculated using first-order pseudo kinetics as follows:

$$\ln \frac{C}{C_0} = K_{app} t \quad (2)$$

where C is the concentration of methylene blue at time t , C_0 is the initial concentration of methylene blue, 10 ppm, and K_{app} is the apparent reaction constant known as the degradation rate. The plots of $\ln(C/C_0)$ versus time for different compositions and photocatalyst loadings of the ZnO/Co/Cs photocatalysts are shown in Fig. 4. Table 2 shows the intercept and degradation rate for various compositions and catalyst loadings of the ZnO/Co/Cs photocatalyst. The results show that 1:1:1 ZnO/Co/Cs at a loading of 3 g has the highest degradation rate among all compositions, as the K_{app} value is 0.24 h⁻¹. The K_{app} value of 1:1 ZnO/Cs, which has no Co, reaches only 0.10 h⁻¹ after 3 g of catalyst loading. This obtained value is a massive difference as the 1:1:1 of ZnO/Co/Cs shows faster degradation and allows good decolourization during photocatalytic degradation. It was concluded that adding Co to the ZnO/Cs photocatalyst accelerates the degradation rate. The Co ions may act as electron scavengers, reducing the recombination of photogenerated electron-hole pairs. It leads to an increase in the number of active species available for photocatalytic degradation.

Table 2 Degradation rate of all composition ZnO/Co/Cs with catalyst loading of 1g, 2g and 3g.

Photocatalyst	Intercept			Degradation Rate (hr ⁻¹)		
	1g	2g	3g	1g	2g	3g
ZnO/Cs (1:1)	0.21	0.22	0.37	0.7	0.05	0.10
ZnO/Co/Cs (1:1:1)	0.18	0.50	0.57	0.03	0.14	0.24
ZnO/Co/Cs (1:2:1)	0.35	0.37	0.98	0.09	0.08	0.19
ZnO/Co /Cs (2:1:1)	0.16	0.31	0.36	0.07	0.06	0.18

4 Conclusions

This work successfully synthesized the different composition ratios of ZnO/Co/Cs photocatalyst beads. The photocatalytic activity of methylene blue using the synthesized ZnO/Co/Cs beads as photocatalyst was investigated by optimizing the various parameters such as composition ratio, irradiation time and catalyst charge. The results focused on the existence of Co as part of the photocatalyst to enhance the photocatalytic activity. The degradation rate of 1:1:1 ZnO/Co/Cs was the best compared to the other three compositions of ZnO/Co/Cs with 0.24 h⁻¹. Compared to the variant without cobalt, the decomposition rate is approx. 0.10 h⁻¹, which corresponds to a difference of approx. 54%. The decolourization percentage was also increased when cobalt was added, especially when using 2 g and 3 g ZnO/Co/Cs photocatalysts.

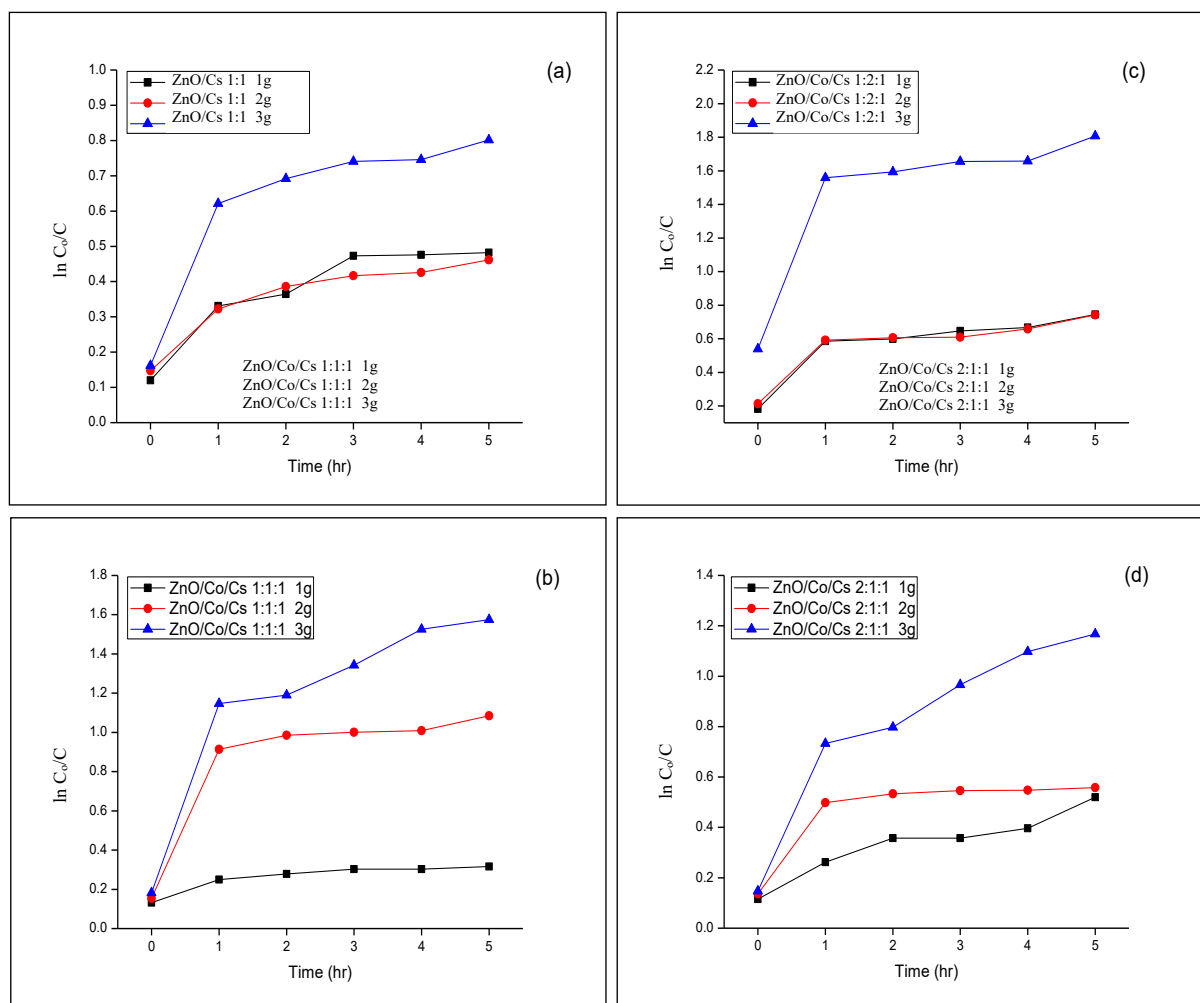


Fig. 4 Plot of $\ln(C_0/C)$ against time at various compositions and catalyst loadings of ZnO/Co/Cs photocatalyst beads (a) 1:1 of ZnO/Cs (b) 1:1:1 of ZnO/Co/Cs (c) 1:2:1 of ZnO/Co/Cs and (d) 2:1:1 of ZnO/Co/Cs.

Declaration of Conflict of Interest

The authors declared no conflict of interest with any other party on the publication of the current work.

ORCID

Mohd Fadhil Majnis  <https://orcid.org/0000-0001-8477-1272>

Mohd Azam Mohd Adnan  <https://orcid.org/0000-0003-0348-7291>

Suhanna Natalya Mohd Suhaimy  <https://orcid.org/0000-0002-0119-8018>

References

- [1] TK Sen, Application of Synthesized Biomass Bamboo Charcoal–Iron Oxide "BC/Fe" Nanocomposite Adsorbents in the Removal of Cationic Methylene Blue Dye Contaminants from Wastewater by Adsorption, *Sustainability* 15(11) (2023) 8841. <https://doi.org/10.3390/su15118841>.
- [2] H.A. Niaei, M. Rostamizadeh, F. Maasumi, M.J. Darabi, Kinetic, Isotherm, and Thermodynamic Studies of Methylene Blue Adsorption over Metal-doped Zeolite Nano-adsorbent, *Physical Chemistry Research* 9 (2021) 17–30. <https://doi.org/10.22036/pcr.2020.233844.1781>.
- [3] S.W. Lee, H.C. Han, Methylene Blue Application to Lessen Pain: Its Analgesic Effect and Mechanism, *Frontiers in Neuroscience* 15 (2021) 663650. <https://doi.org/10.3389/fnins.2021.663650>.

- [4] T. Saeed, A. Naeem, I.U. Din, M. Farooq, I.W. Khan, M. Hamayun, T. Malik, Synthesis of chitosan composite of metal-organic framework for the adsorption of dyes; kinetic and thermodynamic approach, *Journal of Hazardous Materials* 427 (2022) 127902. <https://doi.org/10.1016/j.jhazmat.2021.127902>.
- [5] P.O. Oladoye, T.O. Ajiboye, E.O. Omotola, O.J. Oyewola, Methylene blue dye: Toxicity and potential elimination technology from wastewater, *Results in Engineering* 16 (2022) 100678. <https://doi.org/10.1016/j.rineng.2022.100678>.
- [6] T. Saeed, A. Naeem, T. Mahmood, Z. Ahmad, M. Farooq, Farida, I.U. Din, I.W. Khan, Comparative study for removal of cationic dye from aqueous solutions by manganese oxide and manganese oxide composite, *International Journal of Environmental Science and Technology* 18 (2021) 659–672. <https://doi.org/10.1007/s13762-020-02844-4>.
- [7] Y. Dadban Shahamat, M. Masihpour, P. Borghei, S. Hoda Rahmati, Removal of azo red-60 dye by advanced oxidation process O₃/UV from textile wastewaters using Box-Behnken design, *Inorganic Chemistry Communication* 143 (2022) 109785. <https://doi.org/10.1016/j.inoche.2022.109785>.
- [8] S. Papić, N. Koprivanac, A.L. Božić, D. Vujević, S.K. Dragičević, H. Kušić, I. Peternel, Advanced Oxidation Processes in Azo Dye Wastewater Treatment, *Water Environment Research* 78 (2006) 572–579. <https://doi.org/10.2175/106143006x101665>.
- [9] S. Song, J. Fan, Z. He, L. Zhan, Z. Liu, J. Chen, X. Xu, Electrochemical degradation of azo dye CI Reactive Red 195 by anodic oxidation on Ti/SnO₂-Sb/PbO₂ electrodes, *Electrochimica Acta* 55 (2010) 3606–3613. <https://doi.org/10.1016/j.electacta.2010.01.101>.
- [10] M. Pal, A. Shrivastava, R.K. Sharma, Wheat straw-based microbial electrochemical reactor for azo dye decolorization and simultaneous bioenergy generation, *Journal of Environmental Management* 323 (2022) 116253. <https://doi.org/10.1016/j.jenvman.2022.116253>.
- [11] M.F. Majnis, O.C. Yee, M.A. Mohd Adnan, M.R. Yusof Hamid, K.Z. Ku Shaari, N. Muhd Julkapli, Photoactive of Chitosan-ZrO₂/TiO₂ thin film in catalytic degradation of malachite green dyes by solar light, *Optical Materials* 124 (2022) 111967. <https://doi.org/10.1016/j.optmat.2022.111967>.
- [12] N. Muhd Julkapli, S. Bagheri, S. Bee Abd Hamid, Recent advances in heterogeneous photocatalytic decolorization of synthetic dyes, *The Scientific World Journal* 2014 (2014). <https://doi.org/10.1155/2014/692307>.
- [13] S. Li, S. Shan, S. Chen, H. Li, Z. Li, Y. Liang, J. Fei, L. Xie, J. Li, Photocatalytic degradation of hazardous organic pollutants in water by Fe-MOFs and their composites: A review, *Journal of Environmental Chemical Engineering* 9 (2021) 105967. <https://doi.org/10.1016/j.jece.2021.105967>.
- [14] X. Chen, Z. Wu, D. Liu, Z. Gao, Preparation of ZnO Photocatalyst for the Efficient and Rapid Photocatalytic Degradation of Azo Dyes, *Nanoscale Research Letters* 12 (2017) 4–13. <https://doi.org/10.1186/s11671-017-1904-4>.
- [15] Y. Lu, Y. Lin, D. Wang, L. Wang, T. Xie, T. Jiang, A high performance cobalt-doped ZnO visible light photocatalyst and its photogenerated charge transfer properties, *Nano Research* 4 (2011) 1144–1152. <https://doi.org/10.1007/s12274-011-0163-4>.
- [16] M.M. Khan, S.F. Adil, A. Al-Mayouf, Metal oxides as photocatalysts, *Journal of Saudi Chemical Society* 19 (2015) 462–464. <https://doi.org/10.1016/j.jscs.2015.04.003>.
- [17] G. Sadanandam, K. Lalitha, V.D. Kumari, M. V. Shankar, M. Subrahmanyam, Cobalt doped TiO₂: A stable and efficient photocatalyst for continuous hydrogen production from glycerol: Water mixtures under solar light irradiation, *International Journal of Hydrogen Energy* 38 (2013) 9655–9664. <https://doi.org/10.1016/j.ijhydene.2013.05.116>.
- [18] M.H. Farzana, S. Meenakshi, Exploitation of zinc oxide impregnated chitosan beads for the photocatalytic decolorization of an azo dye, *International Journal of Biological Macromolecules* 72 (2015) 900–910. <https://doi.org/10.1016/j.ijbiomac.2014.09.038>.
- [19] M. Annaduzzaman, Chitosan biopolymer as an adsorbent for drinking water treatment Investigation on Arsenic and Uranium, 2015.
- [20] M. Vakili, M. Rafatullah, B. Salamatinia, A.Z. Abdullah, M.H. Ibrahim, K.B. Tan, Z. Gholami, P. Amouzgar, Application of chitosan and its derivatives as adsorbents for dye removal from water and wastewater: A review, *Carbohydrate Polymers* 113 (2014) 115–130. <https://doi.org/10.1016/j.carbpol.2014.07.007>.
- [21] S. Çınar, Ü.H. Kaynar, T. Aydemir, S. Çam Kaynar, M. Ayvaci, An efficient removal of RB5 from aqueous solution by adsorption onto nano-ZnO/Chitosan composite beads, *International Journal of Biological Macromolecules* 96 (2017) 459–465. <https://doi.org/10.1016/j.ijbiomac.2016.12.021>.
- [22] M.H. Farzana, S. Meenakshi, Visible light-driven photoactivity of zinc oxide impregnated chitosan beads for the detoxification of textile dyes, *Applied Catalysis A: General* 503 (2015) 124–134. <https://doi.org/10.1016/j.apcata.2014.12.034>.

- [23] D. Bokov, A. Turki Jalil, S. Chupradit, W. Suksatan, M. Javed Ansari, I.H. Shewael, G.H. Valiev, E. Kianfar, Nanomaterial by Sol-Gel Method: Synthesis and Application, *Advances in Materials Science and Engineering* 2021 (2021). <https://doi.org/10.1155/2021/5102014>.
- [24] M.C. García, M. Mora, D. Esquivel, J.E. Foster, A. Rodero, C. Jiménez-Sanchidrián, F.J. Romero-Salguero, Microwave atmospheric pressure plasma jets for wastewater treatment: Degradation of methylene blue as a model dye, *Chemosphere* 180 (2017) 239–246. <https://doi.org/https://doi.org/10.1016/j.chemosphere.2017.03.126>.
- [25] X. Guo, Z. Ma, Y. Yuan, Y. Kang, H. Xu, Z. Mao, Y. Ma, Photoinduced Absorption Spectroscopy of Photoelectrocatalytic Methylene Blue Oxidation on Titania and Hematite: The Thermodynamic and Kinetic Impacts on Reaction Pathways, *Advanced Science* 10 (2023) 1–11. <https://doi.org/10.1002/advs.202206685>.
- [26] R. Ballesteros-Garrido, R. Adam, Zinc Oxide (ZnO): an Amphoteric Metal Oxide with Dehydrogenating Activity, *SynOpen* 07 (2023) 142–144. <https://doi.org/10.1055/a-2063-4007>.
- [27] A. Jaswal, K. Kishore, A. Singh, J. Singh, S. Dixit, K. Kumar, M.K. Sinha, Synthesis and Characterization of Highly Transparent and Superhydrophobic Zinc Oxide (ZnO) Film, in: C. Prakash, S. Singh, G. Krolczyk (Eds.), *Adv. Funct. Smart Mater.*, Springer Nature Singapore, Singapore, 2023: pp. 119–127.
- [28] I. Bilican, S. Pekdemir, M.S. Onses, L. Akyuz, E.M. Altuner, B. Koc-Bilican, L.-S. Zang, M. Mujtaba, P. Mulerčikas, M. Kaya, Chitosan Loses Innate Beneficial Properties after Being Dissolved in Acetic Acid: Supported by Detailed Molecular Modeling, *ACS Sustainable Chemistry & Engineering* 8 (2020) 18083–18093. <https://doi.org/10.1021/acssuschemeng.0c06373>.
- [29] P. Wulan, Y. Kusumastuti, A. Prasetya, Removal of Fe (II) from Aqueous Solution by Chitosan Activated Carbon Composite Beads, in: *Ind. Waste Management*, Trans Tech Publications Ltd, 2020: pp. 3–8. <https://doi.org/10.4028/www.scientific.net/AMM.898.3>.
- [30] A.M. Gueli, G. Bonfiglio, S. Pasquale, S.O. Troja, Effect of particle size on pigments colour, *Color Research & Application* 42 (2017) 236–243. <https://doi.org/10.1002/col.22062>.
- [31] B. Vasecharan, J. Sivakamavalli, R. Thaya, Synthesis and characterization of chitosan-ZnO composite and its antibiofilm activity against aquatic bacteria, *Journal of Composite Materials* 49 (2015) 177–184. <https://doi.org/10.1177/0021998313515289>.
- [32] V. Gandhi, R. Ganesan, H.H. Abdulrahman Syedahamed, M. Thaiyan, Effect of Cobalt Doping on Structural, Optical, and Magnetic Properties of ZnO Nanoparticles Synthesized by Coprecipitation Method, *The Journal of Physical Chemistry C* 118 (2014) 9715–9725. <https://doi.org/10.1021/jp411848t>.
- [33] S. Chen, K. Zhang, Z. Li, Y. Wu, B. Zhu, J. Zhu, Hydrogen-bonded supramolecular adhesives: Synthesis, responsiveness, and application, *Supramolecular Materials* 2 (2023) 100032. <https://doi.org/10.1016/j.supmat.2023.100032>.
- [34] Z. Zhu, Y. Niu, S. Wang, M. Su, Y. Long, H. Sun, W. Liang, A. Li, Magnesium hydroxide coated hollow glass microspheres/chitosan composite aerogels with excellent thermal insulation and flame retardancy, *Journal of Colloid and Interface Science* 612 (2022) 35–42. <https://doi.org/10.1016/j.jcis.2021.12.138>.